CHAPTER IV
RESULTS AND DISCUSSION

4.1 Adsorbent Characterizations

4.1.1 Zeta Potential Measurements

The zeta potential of all samples as a function of pH (pH_{pzc}) and their total surface acidity obtained by Boehm method are shown in Table 4.1. The CSAC – Untreated has a pH_{pzc} of 4.5 when the zeta potential is 0 mV. The value shifts below 3.5 when the sample is treated with acids and over 7.0 with the alkali treatment.

Table 4.1 Zeta potential measurements of activated carbon

Adsorbents	pH_{pzc}	Adsorbents	pH_{pzc}
CSAC	4.5	CSAC/H_2SO_4	3.3
CSAC/KOH	7.6	CSAC/HNO_3	2.5
CSAC/NaOH	7.5	CSAC/H_3PO_4	2.7
CSAC/NH_4OH	7.3		

4.1.2 Surface Area Analysis

Activated carbons used in the study were produced from different biomass sources and chemical surface treatment, which inherently affect their ability to adsorb methane and carbon dioxide. Nitrogen adsorption-desorption isotherms of the adsorbents were conducted using an Autosorb-1MP (Quantachrome Instrument). The adsorbents were previously degassed at 250 °C, and the study was carried out at liquid nitrogen temperature, -196 °C. The specific surface area was calculated with the Brunauer, Emmet, and Teller (BET) method, and the pore size distribution was obtained by Dubinin-Radushkevic, DR method. The total pore volume was estimated from the adsorption of nitrogen at the relative pressure of 0.99. In this study, CSAC is referred to coconut shell activated carbon.

Table 4.2 BET surface area, micropore volume, and average pore diameter of investigated adsorbents

Adsorbent	Physical Characterization			
	BET Surface area (m^2/g)	Micropore volume (cm^3/g)	Total pore volume (cm^3/g)	Average pore diameter (Å)
CSAC	1,012	0.54	0.56	22.35
CSAC/KOH	900	0.48	0.50	22.29
CSAC/NaOH	1,019	0.55	0.57	22.20
CSAC/NH_4OH	1,022	0.55	0.57	22.15
CSAC/H_2SO_4	996	0.53	0.55	22.26
CSAC/HNO_3	988	0.53	0.55	22.30
CSAC/H_3PO_4	922	0.49	0.51	22.28

Table 4.2 summarizes the BET surface area, total pore volume, micropore volume, and average pore diameter of the adsorbents. The BET surface area of CSAC treated by acid/base, the surfaces from the CSAC modified by alkalis are 1,022 m^2/g for CSAC/NH_4.OH and 1,019 m^2/g CSAC/NaOH. They have selectively higher BET surface areas than other acid–treated samples. In contrast, the surface areas of acid-treated CSAC range from 900 to 996 m^2/g, which are lower than that of the original CSAC (1,012 m^2/g). Normally, the acid or base treatment does not affect the CSAC surface properties. After the treatment by strong acid or base, the surface area of the activated carbon decreases. This result may be due to the collapse of pore structure. Similarly, the CSAC/KOH shows the decrease in surface area. The decrease in the surface area of the CSAC/H_3PO_4 indicates that micropore wall breaking after the treatment with a strong oxidant. On the other hand, the CSAC treated by alkali could develop surface area and create micropore volume. Alcañiz-

Monge *et al.* (1997) and Lozano-Castello *et al.* (2002) reported that micropore is the size of porosity useful for methane storage applications.

4.1.3 Scanning Electron Microscopy

SEM, Hitachi S-4800, was used to investigate the morphology of the CSAC with the applied voltage at 15 kV and using magnification of 15,000, as shown in Figure 4.1.

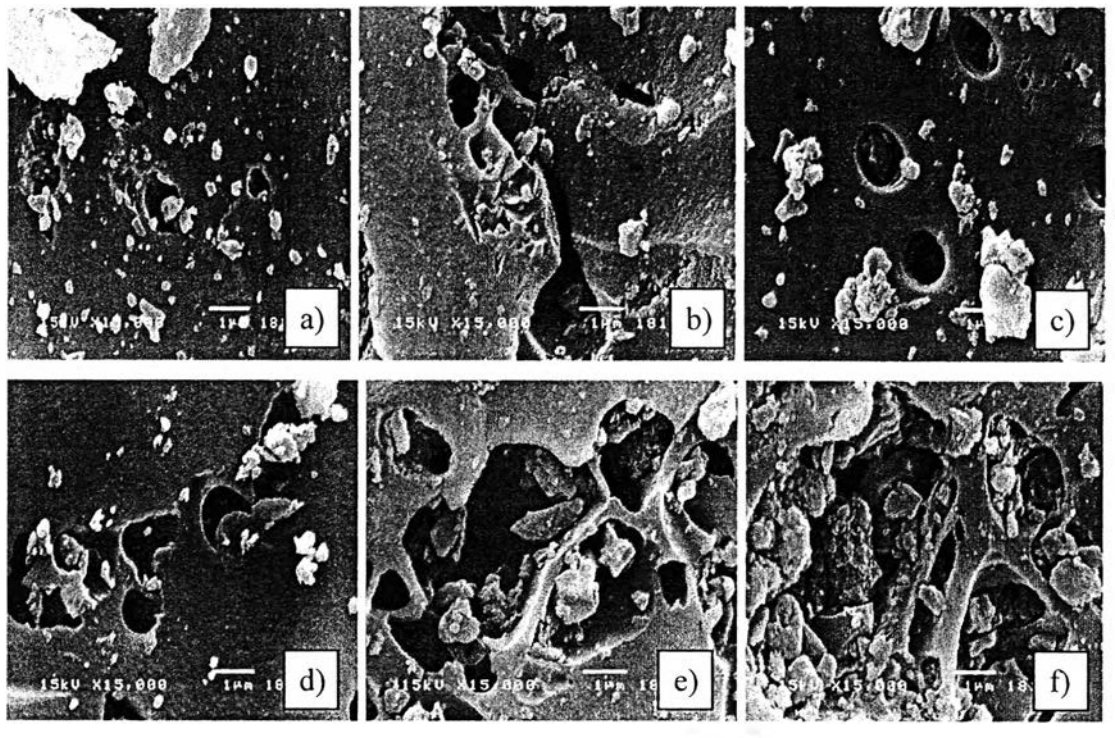

Figure 4.1 SEM micrographs of alkali or acid treated CSAC: a) CSAC; b) CSAC/NH_4OH; c) CSAC/NaOH; d) CSAC/H_2SO_4; e) CSAC/H_3PO_4; f) CSAC/HNO_3.

The SEM micrographs of alkali or acid treated CSAC are shown in Figure 4.1. The CSAC modified by NaOH exhibits a purified surface. Various pore sizes can be observed on the surface and inside the particle. The surfaces of the CSAC are similar, although some pores are blocked. Both the surface and pore structure of the CSAC treated with acids are partially destroyed or enlarged, which greatly decreases the BET surface area.

4.1.4 IR Spectrum Analysis

Fourier transform infrared spectroscopy (FTIR) was used to qualitatively evaluate the chemical structure of carbon materials. The IR spectra were collected using a Nicolet, Nexus 670 FTIR spectrometer. The activated carbon samples were grounded into fine powder and mixed with KBr. The mixture was used for the preparation of KBr pellets. The IR spectrum was obtained over a frequency between 400 and 4,000 cm^{-1}. The FTIR spectra for tested activated carbons were recorded to obtain better insight on the function groups available on the carbon surface. As shown in Table 4.3, all samples exhibit bands at 3,435 and 2,920 cm^{-1}, which are due to surface functional group as hydroxyl (-OH) and asymmetrical and symmetrical stretching of CH_2, respectively. The adsorption band of the cabonyl group (1,558 cm^{-1}) and the phenolic group (1,118 cm^{-1}) can be observed in the CSAC, CSAC/NaOH, CSAC/ NH_4OH, CSAC/H_2SO_4, and CSAC/H_3PO_4. The CSAC/ NH_4OH and CSAC/HNO_3 show the stretching of C=O in cyclic amides at 1,558 cm^{-1} as a result of chemical modification by NH_4OH and HNO_3. Only the CSAC/NaOH, CSAC/HNO_3, and CSAC/H_3PO_4 have the carboxylic group (-COOH) adsorption band, which appears at 1,382-1,392 cm^{-1}.

Table 4.3 IR assignments of functional groups on carbon surfaces

Surface group	Adsorption peaks (cm^{-1})						
	Reference	This work					
		CSAC	CSAC/NaOH	CSAC/ NH_4OH	CSAC/H_2SO_4	CSAC/HNO_3	CSAC/H_3PO_4
-OH	3,435	3,430	3,400	3,408	3,409	3,394	3,436
CH_2	2,920	2,925	2,922	2,925	2,918	2,921	2,923
C=C	1,629	1,633	1,628	1,630	1,629	1,615	1,631
C=O	1,558	-	1,558	1,572	-	1,566	-
COOH	1,382-1,392	-	1,385	-	-	1,390	1,384
COC	1,157	-	-	-	-	1,134	-
COH	1,118	1,115	1,120	1,133	1,118	-	1,130

4.1.5 Methyl Ester Sulfonates Adsorption

Adsorption of methyl ester sulfonates (MES) on the activated carbon as a function of adsorption time is shown in Table 4.4. When the initial MES concentration of 152.8 mg/l was used for the adsorption, the MES concentration decreases to 43.53 mg/l and 30.72 mg/l from 1 to 2 h, after the adsorption. This decrease in the adsorption rate may be due to a distribution of surface sites that cause the decrease in the adsorbent-adsorbate interaction with increasing surface density (Nameni *et al.*, 2008). It may be explained by the fact that the adsorbate molecule attains the equilibrium at time. The adsorption then slows down in later stage because initially a number of vacant surface sites may be available for the adsorption and, after some time, the remaining vacant surface site may be exhausted due to repulsive force between the molecules of adsorbate and counter ion binding at the surface of the adsorbent (Hasan *et al.*, 2000). It can be clearly observed that the adsorption for three hours is sufficient for equilibrium adsorption of MES on the activated carbon.

Table 4.4 Methyl ester sulfonate adsorption as a function of time

MES initial conc. (mg/l)	Time (h)	Concentration after adsorption (mg/l)
152.8	1	43.53
	2	30.72
	3	27.94
	6	27.44
70	1	23.11
	2	16.66
	3	11.44
	6	11.50
50	1	12.09
	2	10.51
	3	10.03
	6	9.934
20	1	6.606
	2	4.870
	3	4.857
	6	4.898
15	1	5.456
	2	2.497
	3	2.230
	6	2.403

Effects of initial MES concentration were studied. The adsorption increases with the increase in the initial concentration, as shown in Table 4.5.

Table 4.5 Adsorption capacity of MES on CSAC

MES initial conc. (mg/l)	MES conc. Before adsorption (mg/l)	MES conc. after adsorption (mg/l)	Adsorption capacity (mg/gm)
160	56.56	28.36	28.2
152.8	57.32	27.94	29.38
152	52.29	33.21	19.08
130	43.54	24.73	18.81
120	38.37	20.05	18.32
110	35.55	17.82	17.73
100	33.35	16.51	16.84
80	26.86	11.29	15.57
70	26.37	11.44	14.93
65	23.51	9.919	13.591
60	21.82	11.92	9.9
50	17.05	10.03	7.02
40	14.33	6.87	7.46
30	9.83	5.20	4.63
20	8.42	4.86	3.56
15	5.44	2.23	3.21
13	0	0	0
6	0	0	0

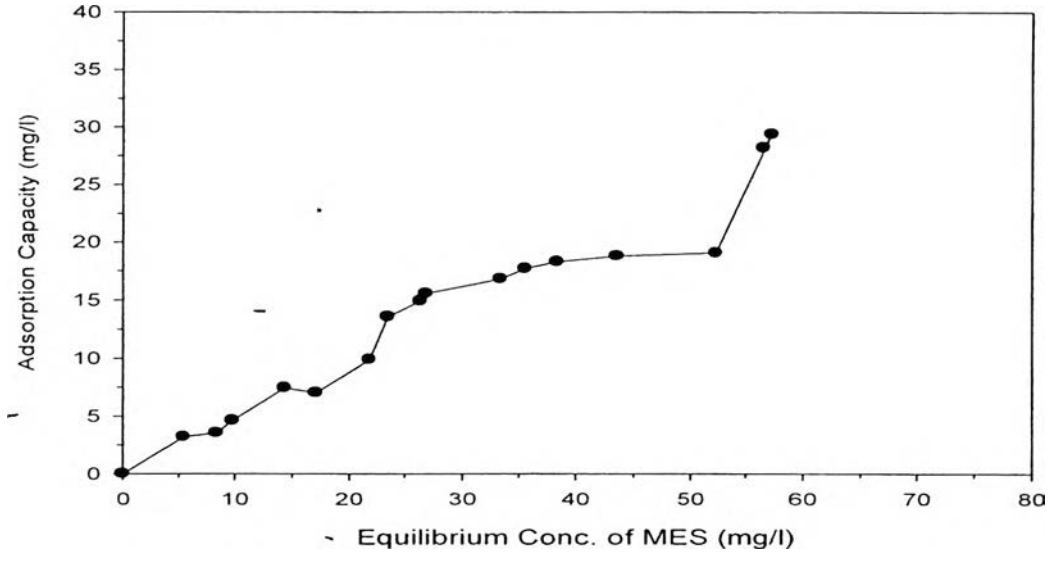

Figure 4.2 Adsorption isotherm of MES on CSAC.

The results from Table 4.5 are plotted and shown in Figure 4.2. The figure shows the unique adsorption isotherm for the adsorption of an anionic surfactant on oppositely charged surfaces. The isotherm is commonly divided into four regions (Patel and Desai, 2011). Region I shows very low adsorption density. In this region, the surfactants are adsorbed as monomers and do not interact with one another. In the present study, Region I is between the concentration range of 6-30 mg/l of MES. Region II is indicated by the sharp increase in the slope isotherm, between 40 and 70 mg/l of MES. In this region, the adsorption is due to the attraction between the ions and the charged solid surface of hydrocarbon chains. The transition from region II to region III is marked by a decrease in the slope of isotherm compared to the transition from region I to II (Somasundaran *et al.*, 1966). In region III, the surfactant ions are probably adsorbed by a slightly different mechanism. The adsorption in this zone is due to the association between the hydrocarbon chains. Region III starts from 70 mg/l of MES. Transition from region III to region IV occurs at the critical micelle concentration (CMC) of the surfactant. Region IV shows the maximum adsorption region, in which the hydrophilic parts to face the aqueous medium (Ginn *et al.*, 1961).

The surfactant molecules adsorbed at a high concentration have a tendency to form bilayer. And because of the hydrophobic reaction between the hydrocarbon chains in this bilayer, it is claimed that the polar groups transform to liquid phase by desorbing (Paulo *et al.*, 1999). Apart from this, hydrophilic reaction, it is also claimed that, at the high concentration, the repulsive forces among the surfactant molecules adsorbed in interface of the solid-solution are effective (Bremmell *et al.*, 1999). However, at the low concentration, a monolayer of MES can be formed resulting in the hydrophobic surface of the activated carbon. In this study, the anionic surfactant were used to treat the activated carbon for methane adsorption.

4.2 Adsorption Experiments

4.2.1 Single Component Adsorption

Investigation on the adsorption kinetics of methane and carbon dioxide was carried out in a stainless steel packed bed column with an inside diameter of 7.0 mm at atmospheric pressure and room temperature. Methane and carbon dioxide composition were varied from 75 to 85 and 5 to 20 vol%, respectively. The breakthrough curves of methane and carbon dioxide were plotted in terms of concentration ratio versus time, as shown in Figures 4.3 and 4.4.

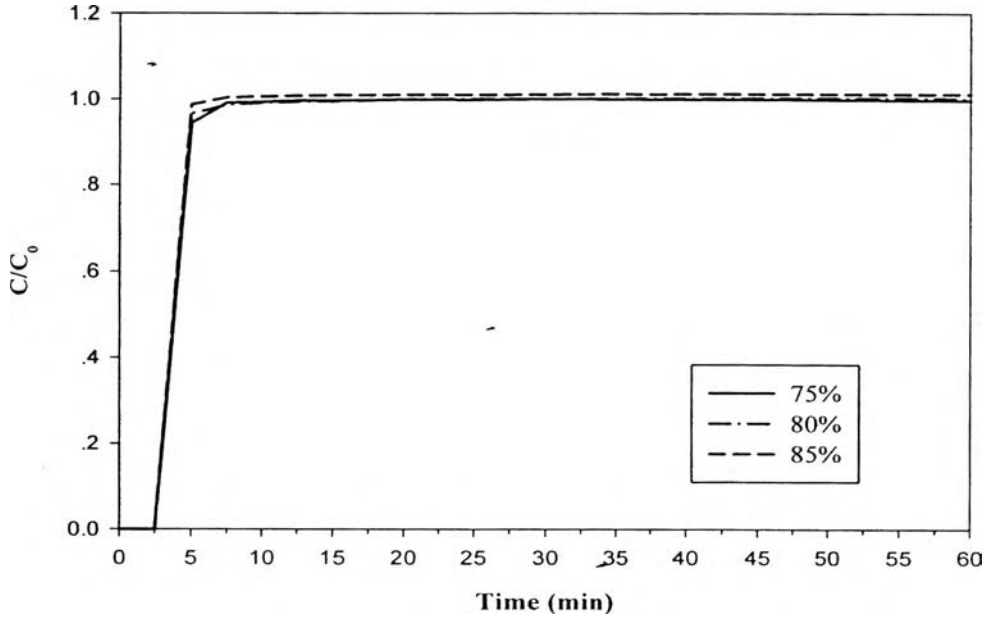

Figure 4.3 Breakthrough curves of methane from the adsorption on the CSAC with the initial concentration of methane at 75, 80, and 85 vol% at room temperature.

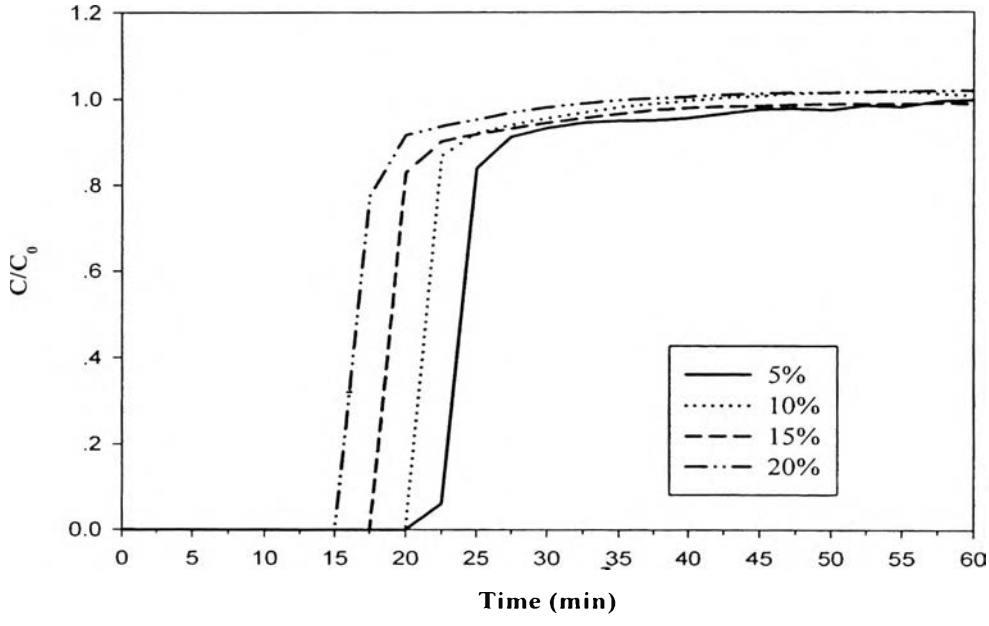

Figure 4.4 Breakthrough curves of carbon dioxide from the adsorption on the CSAC with the initial concentration of carbon dioxide at 5, 10, 15, and 20 vol% at room temperature.

From the methane adsorption, the result shows that the change in the methane concentration from 75 to 85 vol% does not affect the adsorption of methane on the CSAC. In contrast with the carbon dioxide adsorption, the change in its concentration from 5 to 20 vol% significantly affects the adsorption. It can also be seen that, when the concentration of carbon dioxide is increased from 5 to 20 vol%, the eluted time decreases from approximately 20 to 15 min due to faster saturation on the CSAC.

4.2.2 Competitive Adsorption

Methane composition was fixed at 10 vol% and carbon dioxide composition was varied from 10 to 30 vol%. The breakthrough curves of methane and carbon dioxide were plotted in terms of concentration ratio versus time, as shown in Figures 4.5 to 4.8.

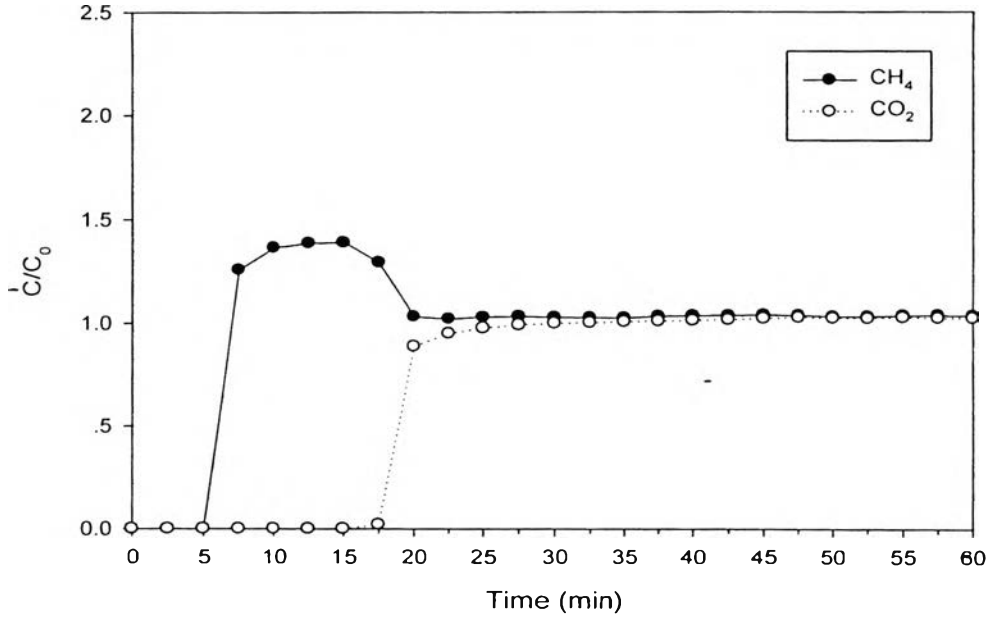

Figure 4.5 Breakthrough curves of methane and carbon dioxide from the competitive adsorption on the CSAC with the initial concentration of methane at 10 vol% and carbon dioxide at 10 vol% at room temperature.

From Figure 4.5, it can be seen that methane breaks through first at about 5 min, followed by carbon dioxide at approximately 17.5 min. Methane roll up can be observed. The roll up reaches the highest concentration ratio at 1.39 before it reverts to the feed concentration at about 20 min. The roll up is commonly observed because of the displacement of a relatively weakly adsorbed component on the CSAC, methane, by a more strongly adsorbed component, carbon dioxide.

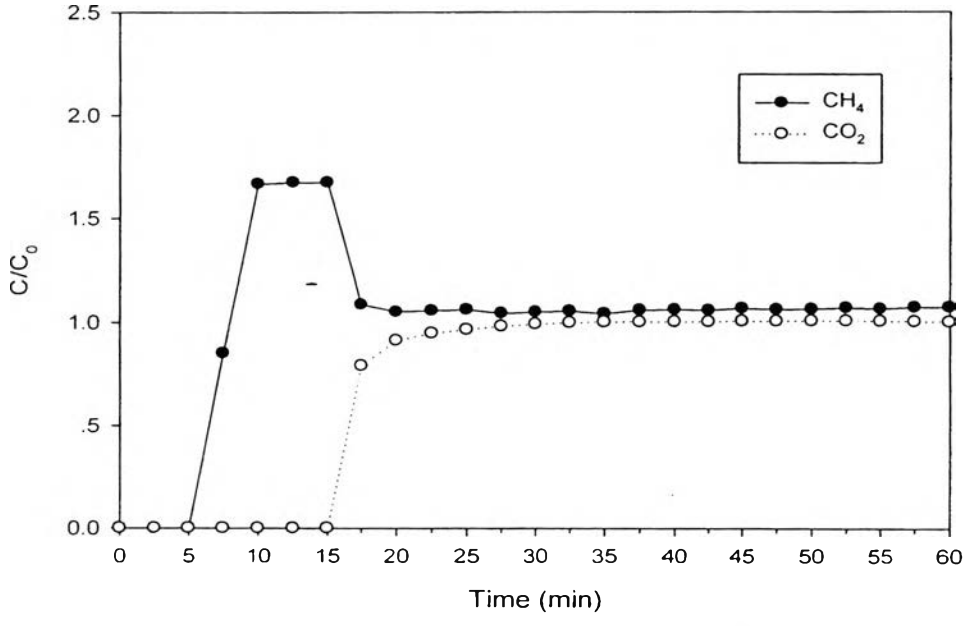

Figure 4.6 Breakthrough curves of methane and carbon dioxide from the competitive adsorption on the CSAC with the initial concentration of methane at 10 vol% and carbon dioxide at 20 vol% at room temperature.

Figure 4.6 shows the breakthrough of methane and carbon dioxide with the initial concentration of 10 and 20 vol%, respectively. From the figure, carbon dioxide breaks through at approximately 15 min, which is faster than that of 10 vol% carbon dioxide (Figures 4.5) due to its higher concentration that gives shorter time to saturate the adsorbent surface than the low carbon dioxide concentration. The roll up reaches the highest concentration ratio at 1.68 before it reverts to the feed concentration at about 17.5 min, which is also faster than that of low carbon dioxide concentration. That is because, when carbon dioxide begins to break through, some methane is re-adsorbed and its gas phase concentration reverts to that of the feed indicating that the bed is saturated with respect to methane.

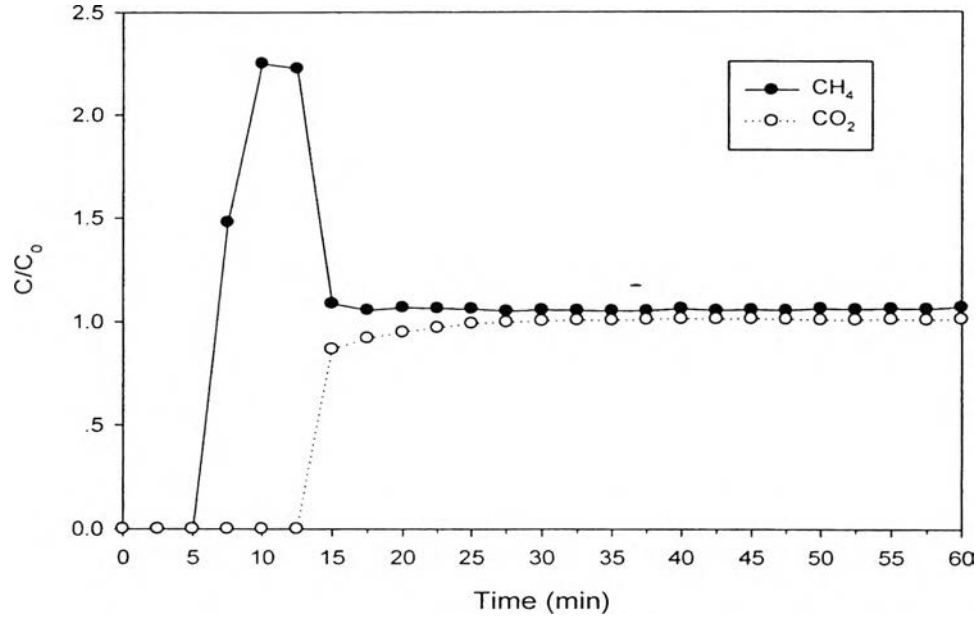

Figure 4.7 Breakthrough curves of methane and carbon dioxide from the competitive adsorption on the CSAC with the initial concentration of methane at 10 vol% and carbon dioxide at 30 vol% at room temperature.

When the carbon dioxide concentration is further increased to 30 vol%, the decrease in the carbon dioxide breakthrough time from 15 to 12.5 min can be observed, as shown in Figures 4.7. The methane roll up also reaches higher concentration ratio with the increase in the carbon dioxide concentration. Again, this is because the higher concentration of more strongly adsorbed component, carbon dioxide, results in the greater displacement of weakly adsorbed component, methane.

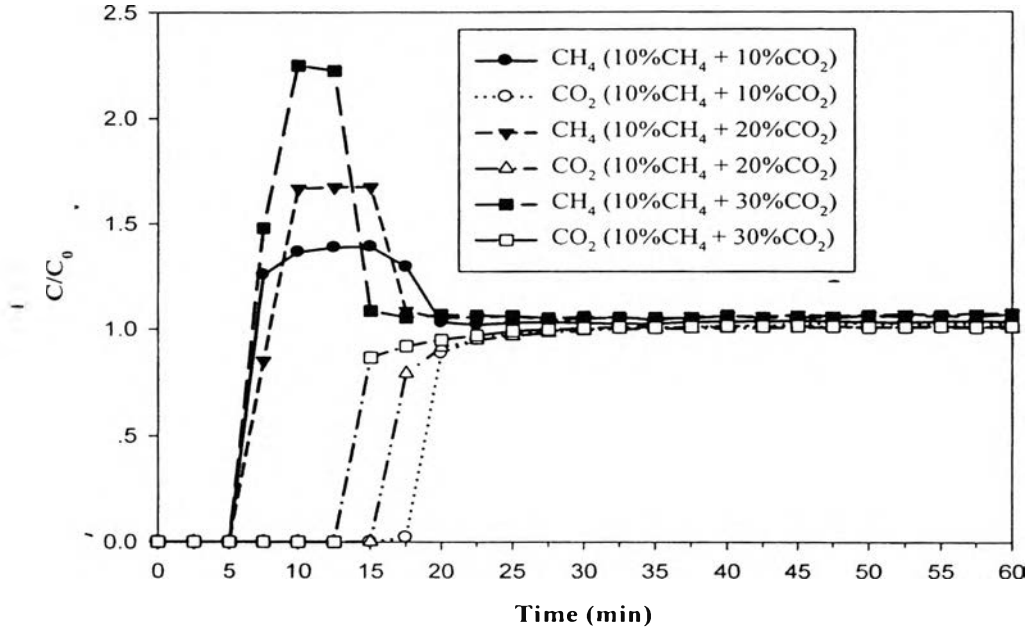

Figure 4.8 Breakthrough curves of methane and carbon dioxide from the competitive adsorption on the CSAC with the initial concentration of methane at 10 vol% and carbon dioxide at 10, 20, and 30 vol% at room temperature.

From Figure 4.8, the weakly adsorbed component, methane, breaks through first at about 5 min. Some of methane is displaced from the adsorbent to give a higher gas phase concentration than was originally present in the feed. As carbon dioxide then begins to break through, some methane is re-adsorbed and its gas phase concentration reverts to that of the feed indicating that the bed is saturated with respect to methane. The displacement of a relatively weakly adsorbed component, methane, by a more strongly adsorbed component, carbon dioxide, is sometimes referred to a roll up effect. In other words, methane roll up increases from the methane concentration ratio of 1.39 to 2.25 with the increase in the concentration of carbon dioxide from 10 to 30 vol%. It can be seen that carbon dioxide more strongly and selectively adsorbs on the activated carbon than methane. It is because the lower surface diffusivity of carbon dioxide is associated with its higher affinity towards the carbon surface. The adsorbed methane molecule has smaller energy barrier than carbon dioxide does, and this could be due to the quadrupole moment of carbon

dioxide compared to the non-polar nature of the methane molecule (Prasetyo and Do, 1998).

4.2.3 Adsorbent Stability

The adsorbent stability was also studied by the 3-cycle adsorption-desorption process of methane and carbon dioxide on the untreated CSAC, CSAC treated by sulfuric acid, CSAC treated by nitric acid, CSAC treated by phosphoric, CSAC treated by potassium hydroxide, CSAC treated by sodium hydroxide, and CSAC treated by Ammonia at atmospheric pressure and room temperature with the same initial concentration of methane and carbon dioxide at 10 and 10 vol%, respectively. The breakthrough curves and desorption cycles of methane and carbon dioxide on the investigated adsorbents for the three cycles are shown in Figures 4.9 to 4.22.

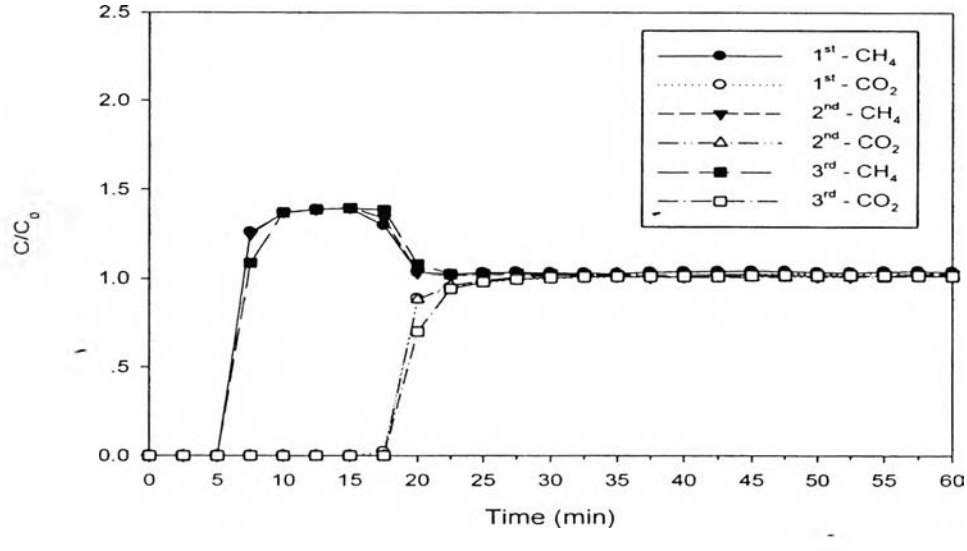

Figure 4.9 Breakthrough curves of methane and carbon dioxide from the 3-cycle adsorption process on untreated CSAC with the initial concentration of methane at 10 vol% and carbon dioxide at 10 vol% at room temperature.

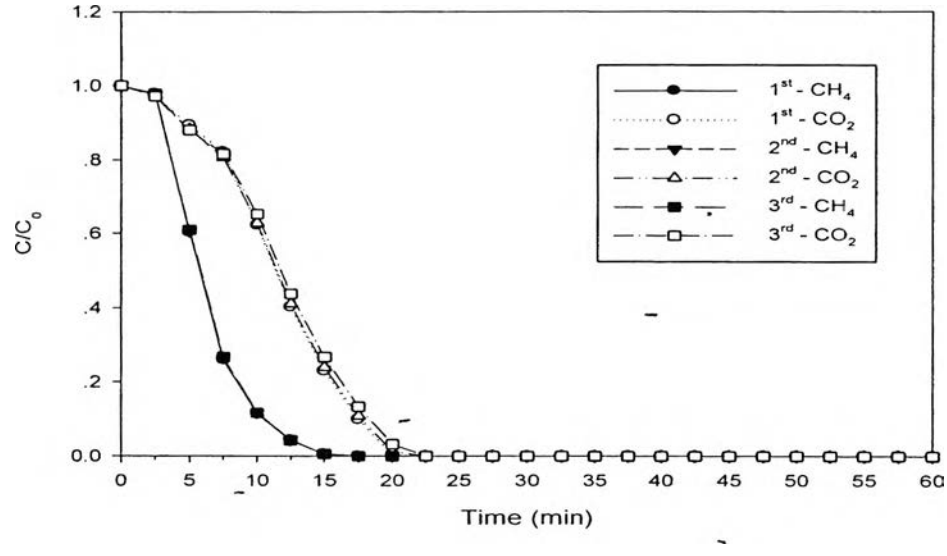

Figure 4.10 Three desorption cycles of methane and carbon dioxide from the CSAC with the initial concentration of methane at 10 vol% and carbon dioxide at 10 vol% at room temperature.

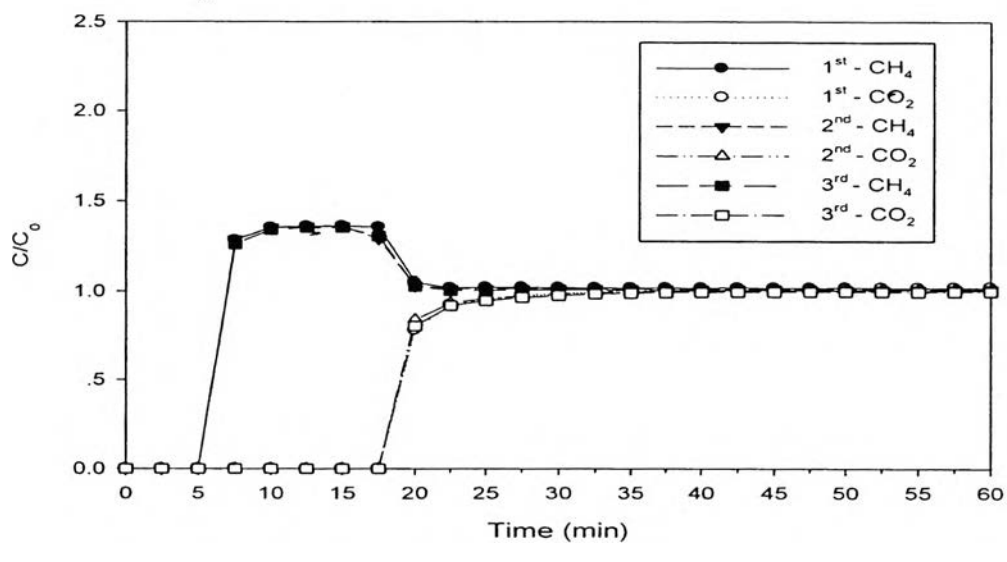

Figure 4.11 Breakthrough curves of methane and carbon dioxide from the 3-cycle adsorption process on the CSAC treated by sodium hydroxide with the initial concentration of methane at 10 vol% and carbon dioxide at 10 vol% at room temperature.

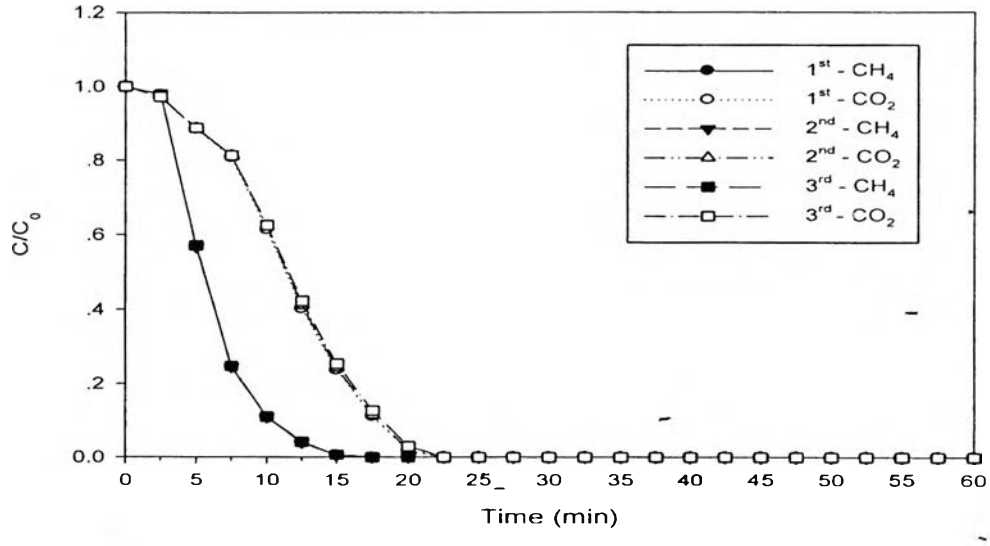

Figure 4.12 Three desorption cycles of methane and carbon dioxide from the CSAC treated by sodium hydroxide with the initial concentration of methane at 10 vol% and carbon dioxide at 10 vol% at room temperature.

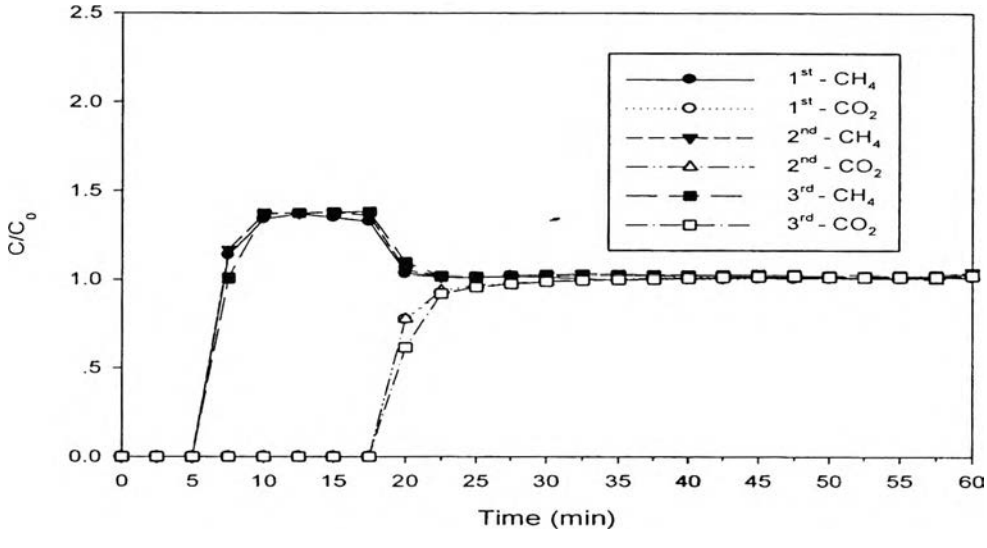

Figure 4.13 Breakthrough curves of methane and carbon dioxide from the 3-cycle adsorption process on the CSAC treated by ammonium hydroxide with the initial concentration of methane at 10 vol% and carbon dioxide at 10 vol% at room temperature.

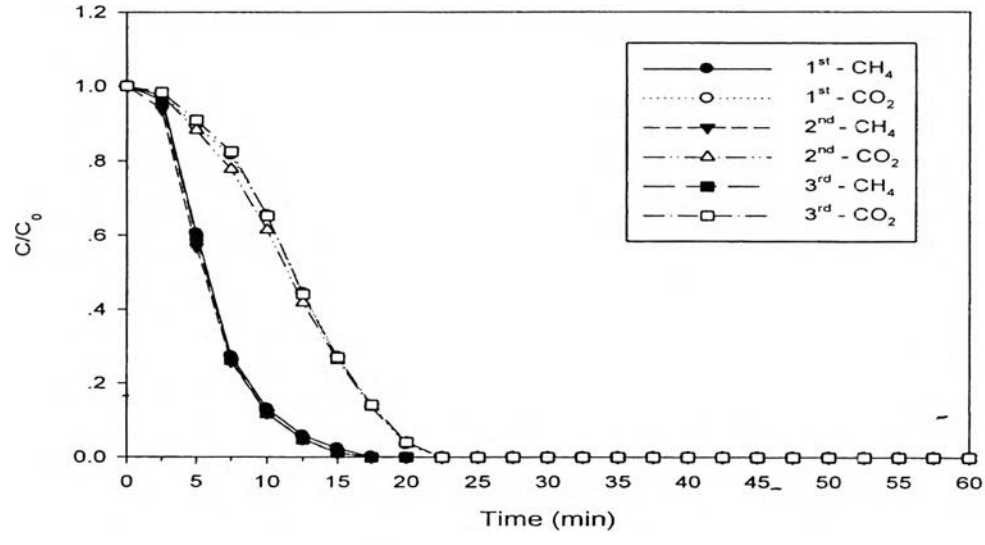

Figure 4.14 Three desorption cycles of methane and carbon dioxide from the CSAC treated by ammonium hydroxide with the initial concentration of methane at 10 vol% and carbon dioxide at 10 vol% at room temperature.

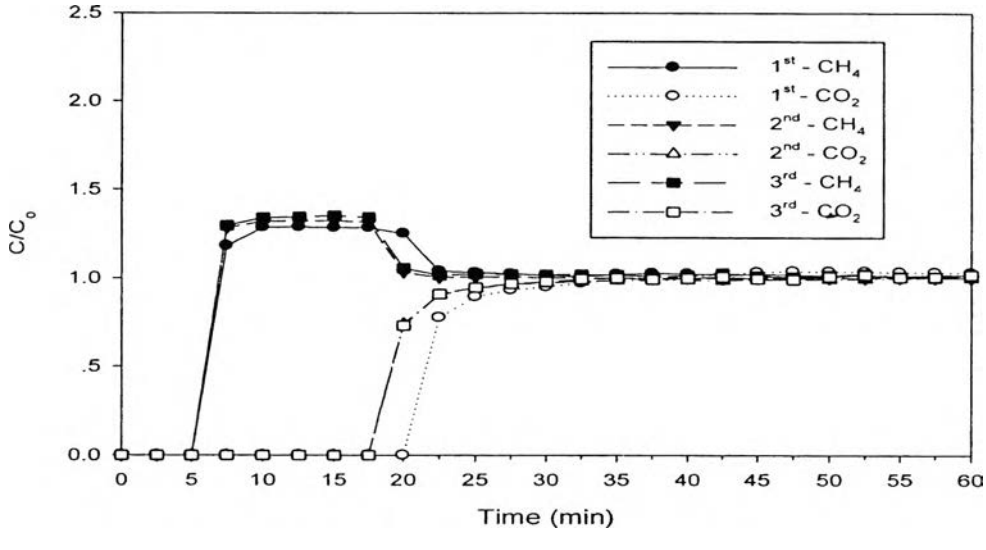

Figure 4.15 Breakthrough curves of methane and carbon dioxide from the 3-cycle adsorption process on the CSAC treated by potassium hydroxide with the initial concentration of methane at 10 vol% and carbon dioxide at 10 vol% at room temperature.

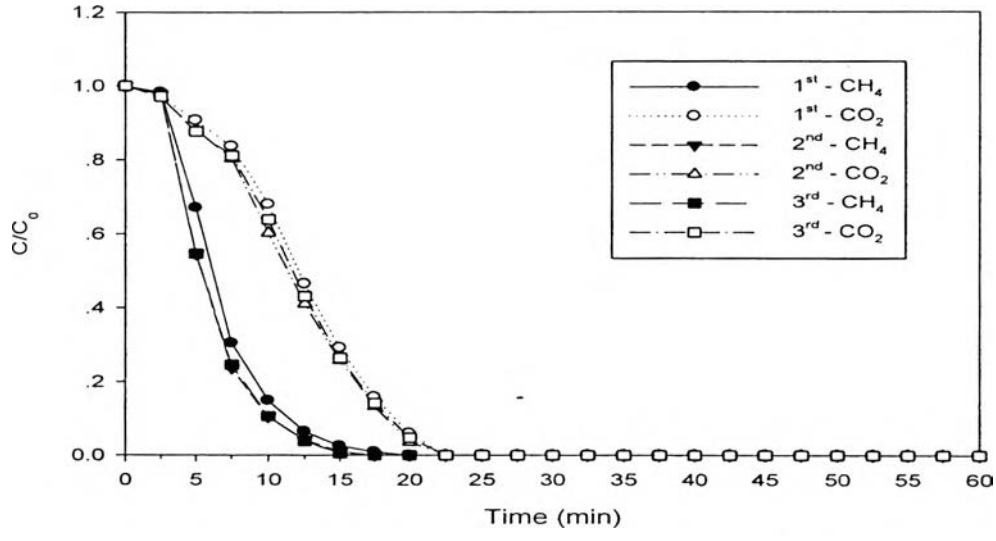

Figure 4.16 Three desorption cycles of methane and carbon dioxide from the CSAC treated by potassium hydroxide with the initial concentration of methane at 10 vol% and carbon dioxide at 10 vol% at room temperature.

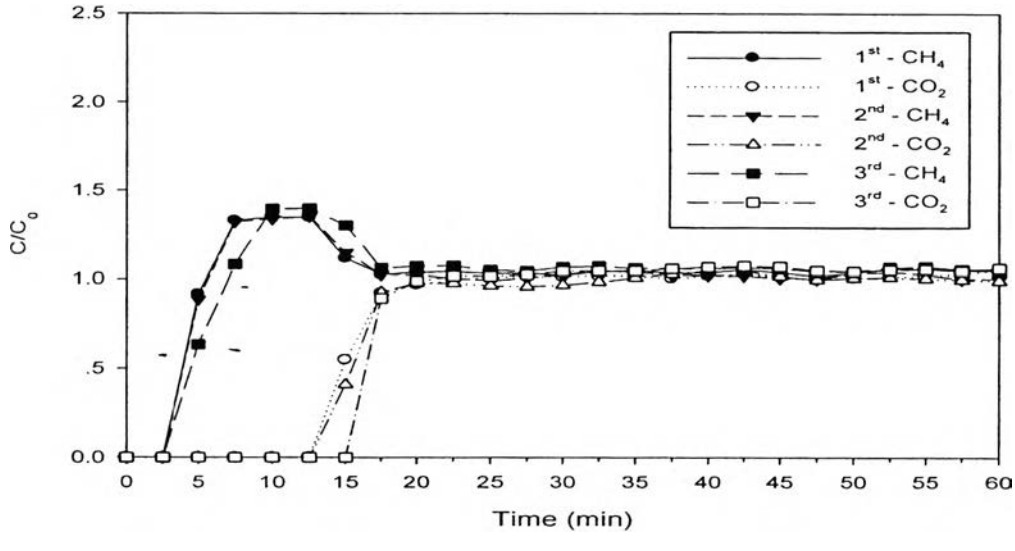

Figure 4.17 Breakthrough curves of methane and carbon dioxide from the 3-cycle adsorption process on the CSAC treated by sulfuric acid with the initial concentration of methane at 10 vol% and carbon dioxide at 10 vol% at room temperature.

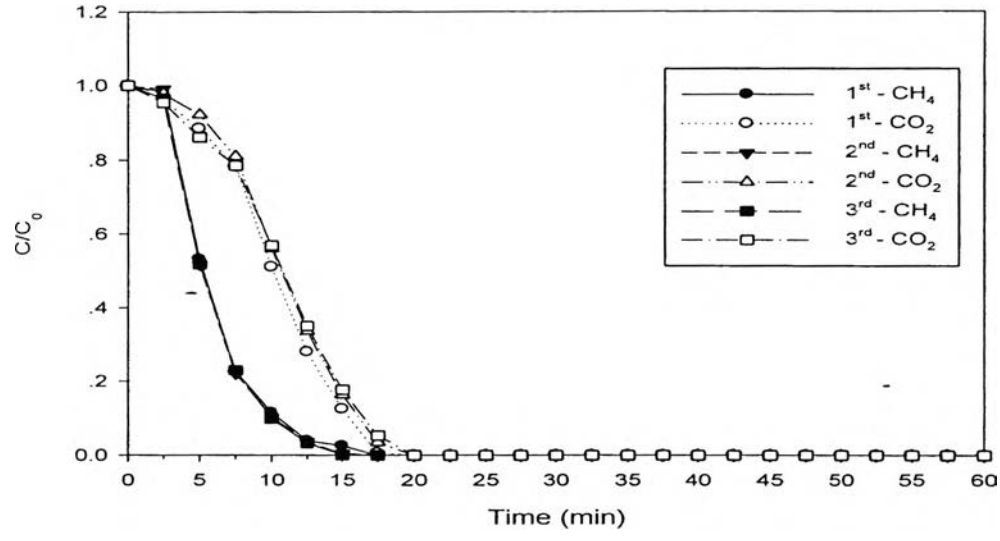

Figure 4.18 Three desorption cycles of methane and carbon dioxide from the CSAC treated by sulfuric acid with the initial concentration of methane at 10 vol% and carbon dioxide at 10 vol% at room temperature.

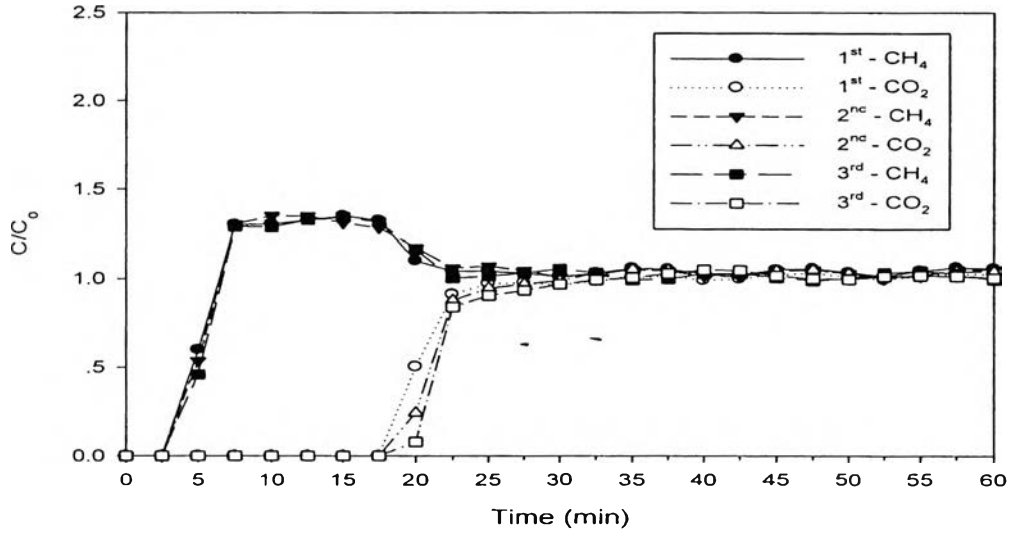

Figure 4.19 Breakthrough curves of methane and carbon dioxide from the 3-cycle adsorption process on the CSAC treated by nitric acid with the initial concentration of methane at 10 vol% and carbon dioxide at 10 vol% at room temperature.

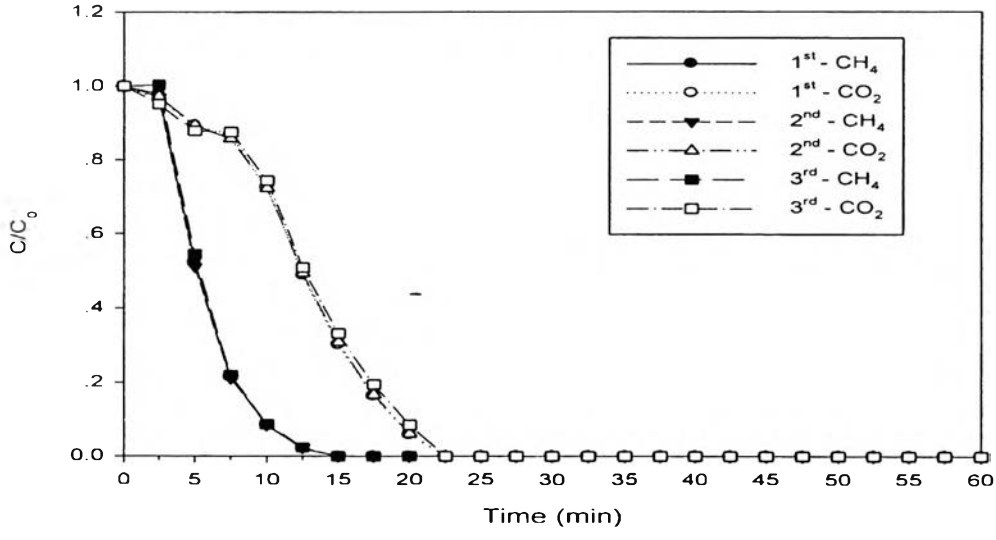

Figure 4.20 Three desorption cycles of methane and carbon dioxide from the CSAC treated by nitric acid with the initial concentration of methane at 10 vol% and carbon dioxide at 10 vol% at room temperature.

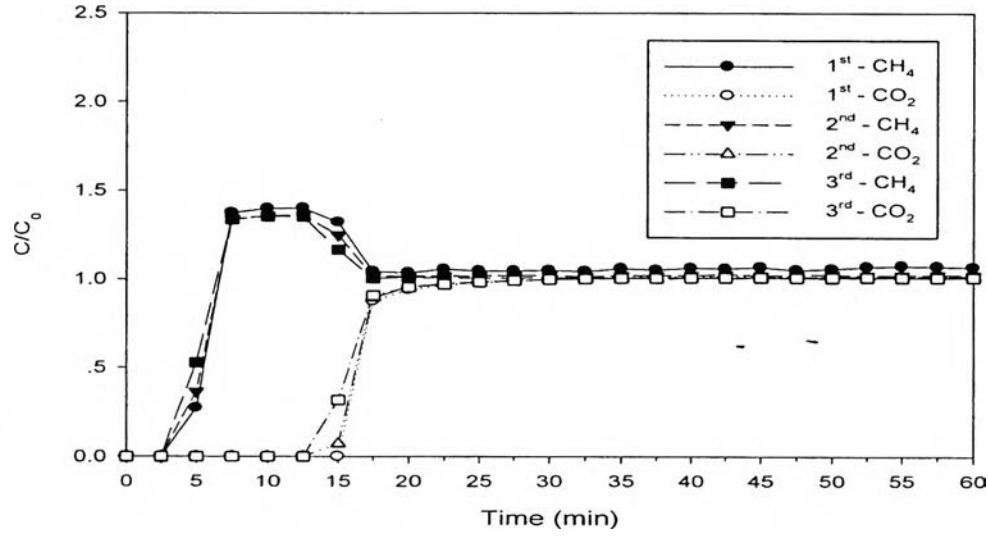

Figure 4.21 Breakthrough curves of methane and carbon dioxide from the 3-cycle adsorption process on the CSAC treated by phosphoric acid with the initial concentration of methane at 10 vol% and carbon dioxide at 10 vol% at room temperature.

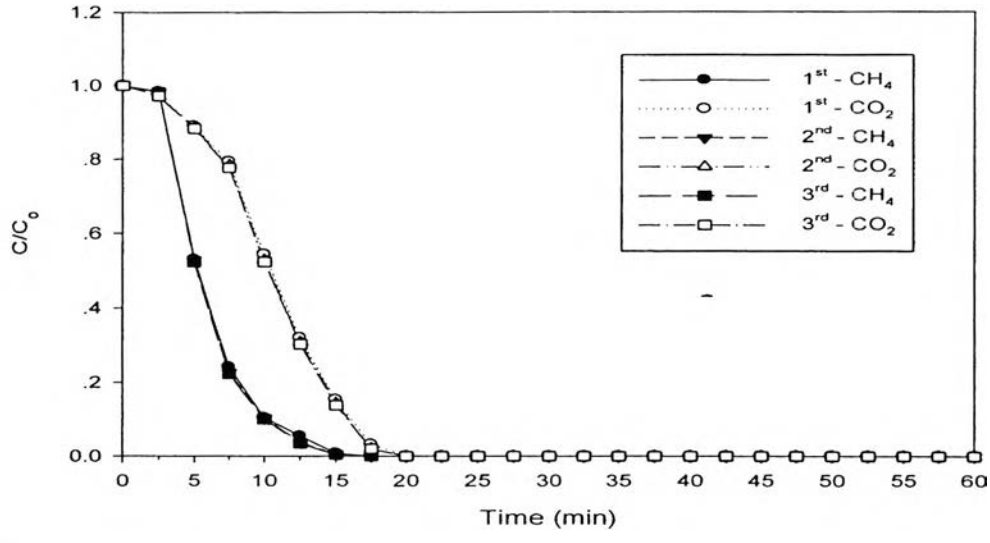

Figure 4.22 Three desorption cycles of methane and carbon dioxide from the CSAC treated by phosphoric acid with the initial concentration of methane at 10 vol% and carbon dioxide at 10 vol% at room temperature.

The adsorption – desorption cycles of methane and carbon dioxide from the regenerated adsorbents shows the same breakthrough patterns for all adsorbents. The results indicate that the stability of the untreated CSAC, CSAC treated by sodium hydroxide, and CSAC treated by ammonium hydroxide is hardly affected with the increase in the adsorption cycle, as seen in Figures 4.9, 4.11, and 4.13 respectively. It has no difference in the breakthrough curves and the breakthrough times of both gases during its regeneration cycles. This could be due to its cleaner surface after the treatment that allows the feed gas molecules to adsorb and desorb easily. It is likely that no gas molecules remain and block the active pores after the regeneration cycles. In contrast, the stability of CSAC treated by potassium hydroxide, CSAC treated by sulphuric acid, CSAC treated by nitric acid, and CSAC treated by phosphoric acid is slightly affected when the adsorption cycle is increased. The breakthrough times of methane and carbon dioxide increase due to the adsorbent lost its ability to adsorb gases. Some gas molecules may block the pores resulting in a longer time to equilibrate its surface. Another reason may be because the adsorbed

carbon dioxide molecules, which preferentially adsorb on all the adsorbents resulting in the change of the adsorbent surface properties.

4.2.4 Comparison of Competitive Adsorption on Different Adsorbents

Various adsorbents including untreated CSAC, CSAC treated by sodium hydroxide, and CSAC treated by ammonium hydroxide, CSAC treated by potassium hydroxide, CSAC treated by sulfuric acid, CSAC treated by nitric acid, and CSAC treated by phosphoric acid were used to study the competitive adsorption of 10 vol% methane and 10 vol% carbon dioxide. The breakthrough curves of methane and carbon dioxide were plotted in terms of concentration ratio versus time, as shown in Figures 4.23 to 4.30.

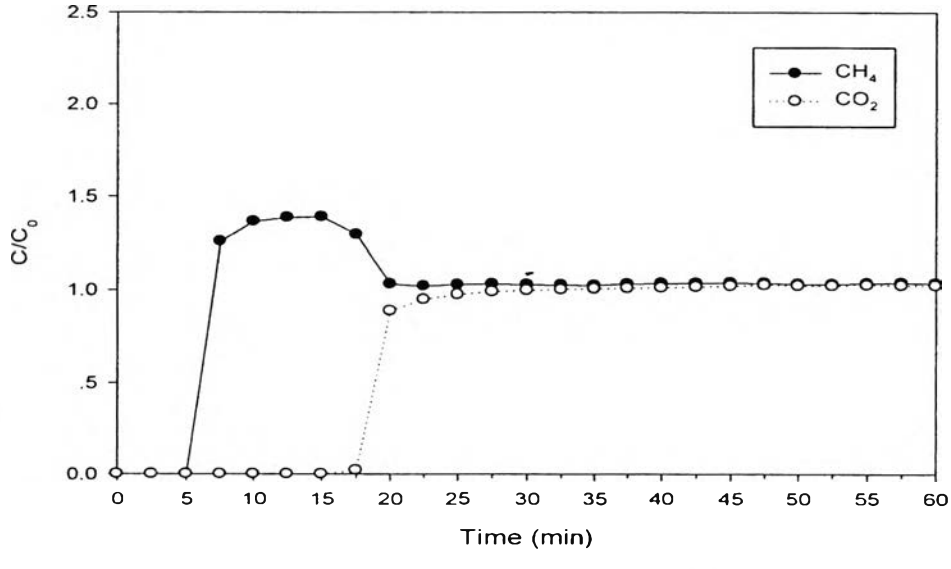

Figure 4.23 Breakthrough curves of methane and carbon dioxide from the competitive adsorption on the untreated CSAC with the initial concentration of methane at 10 vol% and carbon dioxide at 10 vol% at room temperature.

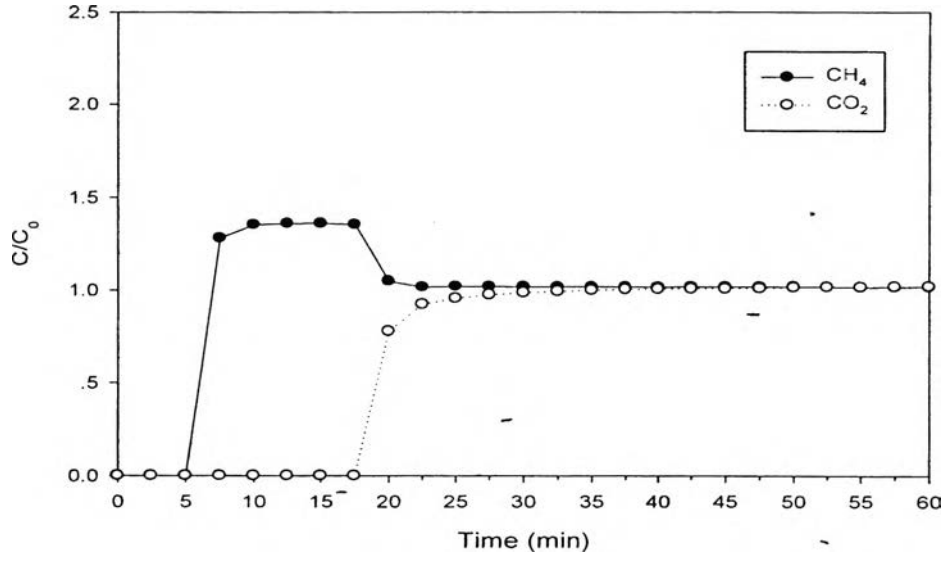

Figure 4.24 Breakthrough curves of methane and carbon dioxide from the competitive adsorption on the CSAC treated by sodium hydroxide with the initial concentration of methane at 10 vol% and carbon dioxide at 10 vol% at room temperature.

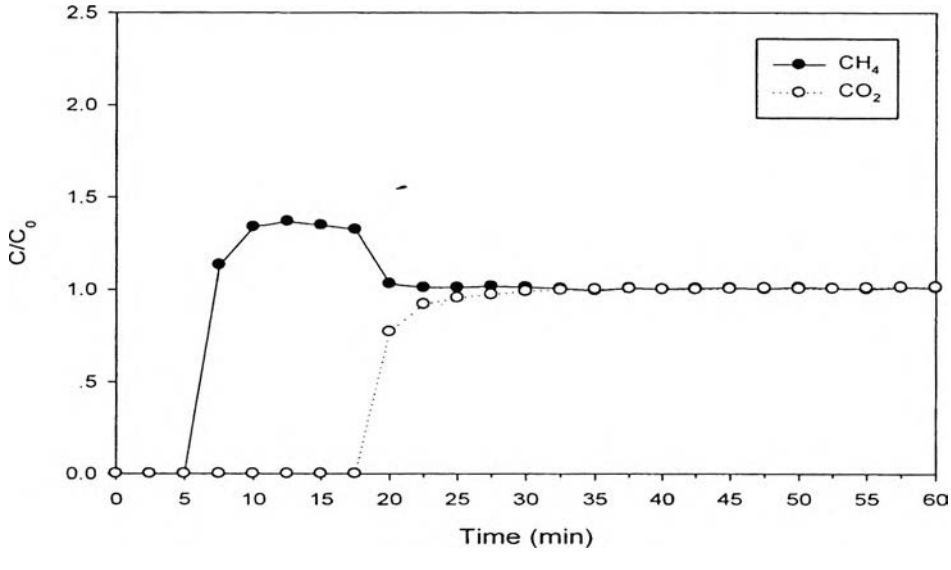

Figure 4.25 Breakthrough curves of methane and carbon dioxide from the competitive adsorption on the CSAC treated by ammonium hydroxide with the initial concentration of methane at 10 vol% and carbon dioxide at 10 vol% at room temperature.

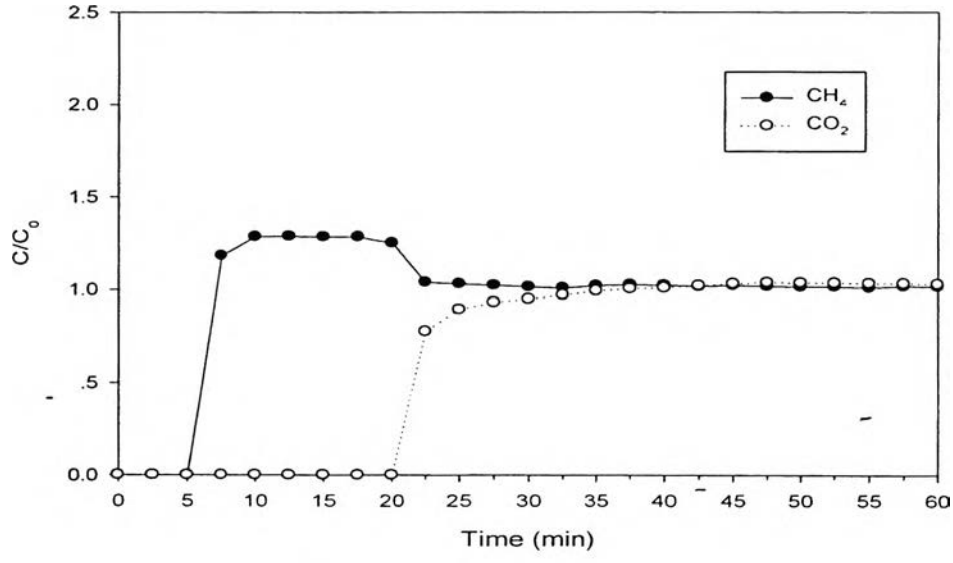

Figure 4.26 Breakthrough curves of methane and carbon dioxide from the competitive adsorption on the CSAC treated by potassium hydroxide with the initial concentration of methane at 10 vol% and carbon dioxide at 10 vol% at room temperature.

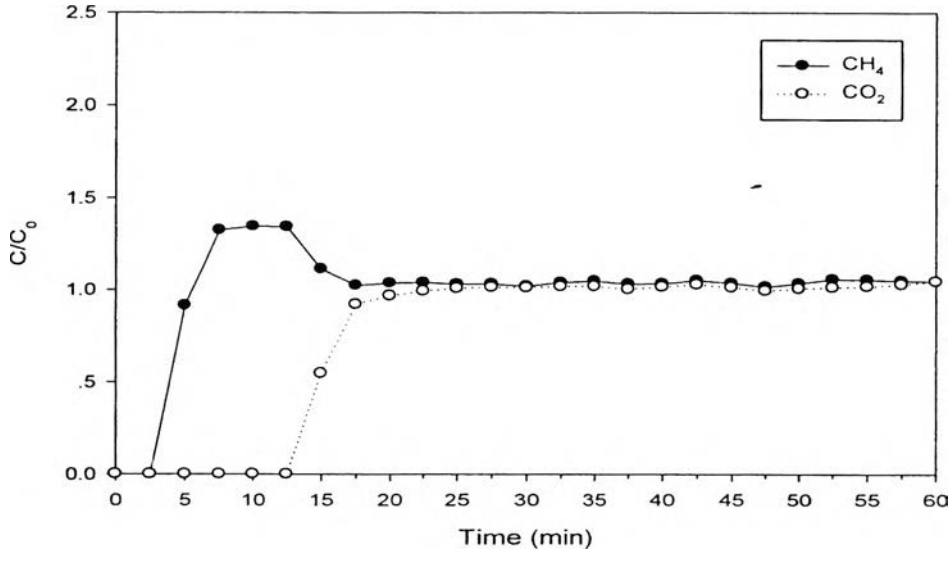

Figure 4.27 Breakthrough curves of methane and carbon dioxide from the competitive adsorption on the CSAC treated by sulfuric acid with the initial concentration of methane at 10 vol% and carbon dioxide at 10 vol% at room temperature.

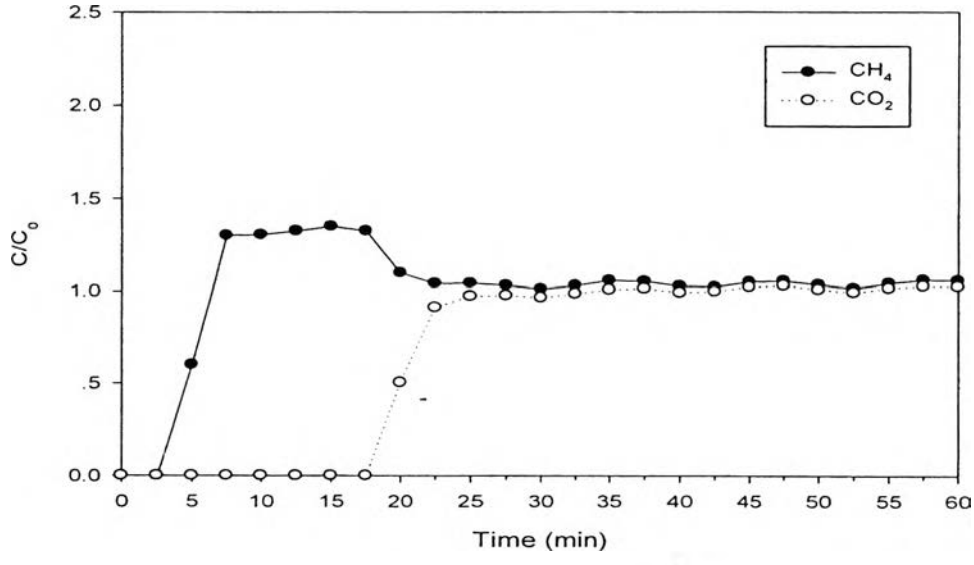

Figure 4.28 Breakthrough curves of methane and carbon dioxide from the competitive adsorption on the CSAC treated by nitric acid with the initial concentration of methane at 10 vol% and carbon dioxide at 10 vol% at room temperature.

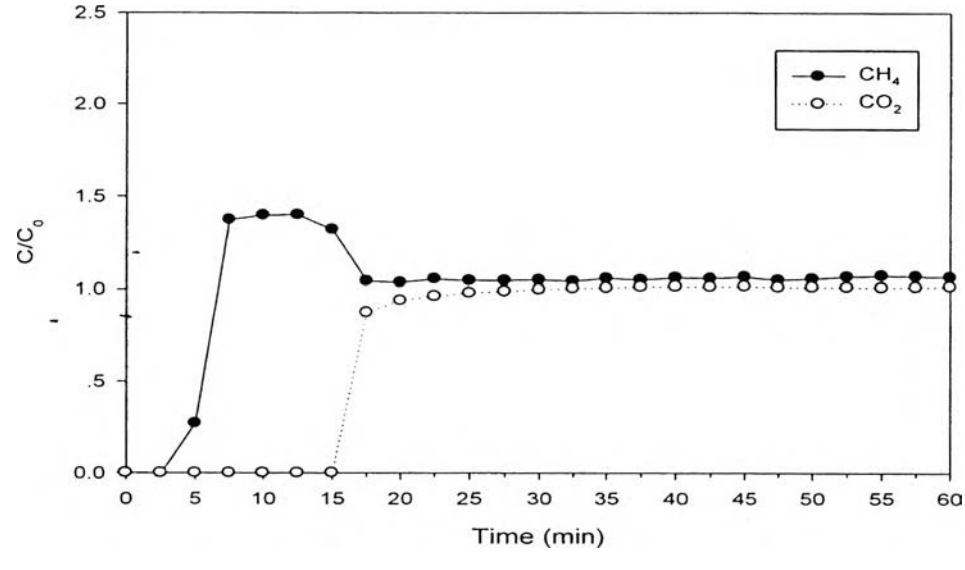

Figure 4.29 Breakthrough curves of methane and carbon dioxide from the competitive adsorption on the CSAC treated by phosphoric acid with the initial concentration of methane at 10 vol% and carbon dioxide at 10 vol% at room temperature.

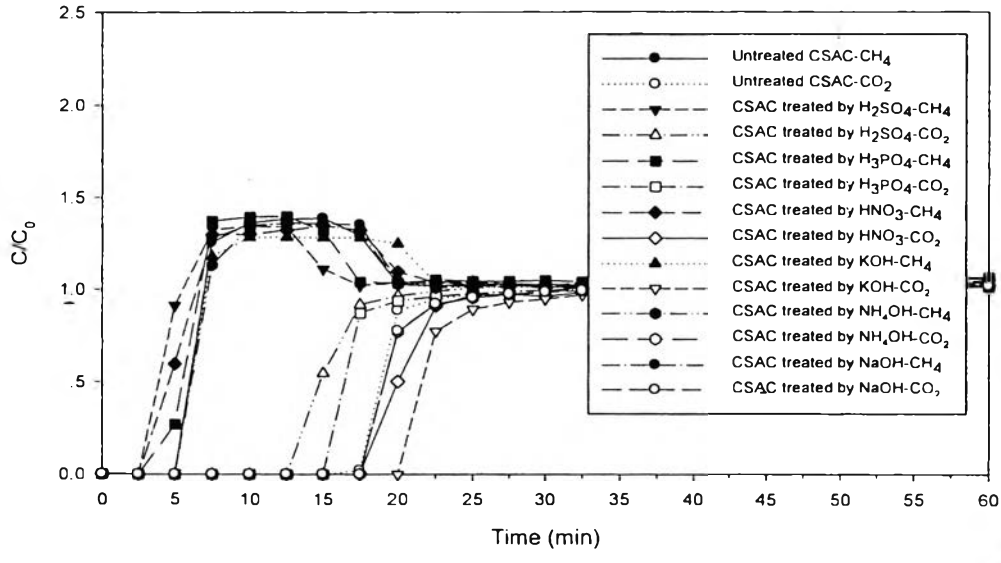

Figure 4.30 Breakthrough curves of methane and carbon dioxide from the competitive adsorption on the untreated CSAC, CSAC treated by sulfuric acid, CSAC treated by phosphoric acid, CSAC treated by nitric acid, CSAC treated by potassium hydroxide, CSAC treated by ammonium hydroxide and CSAC treated by sodium hydroxide with the initial concentration of methane at 10 vol% and carbon dioxide at 10 vol% at room temperature.

For detail comparison of chemical treatment, all the results from Figures 4.23 to 4.29 were plotted in Figure 4.30. From Figure 4.30, it can be seen that methane breaks through first at about 2.5 min from the CSAC treated by sulfuric acid, nitric acid, and phosphoric acid, followed by the untreated CSAC at about 5 min. Methane elutes from the CSAC treated by potassium hydroxide, ammonium hydroxide and sodium hydroxide at the same time as that of the untreated CSAC. The methane roll up reaches the highest concentration ratio at approximately 1.3, which is very similar to all adsorbents. The carbon dioxide breakthrough time is decreased subsequently from the adsorption on the CSAC treated by potassium hydroxide at 20 min, the untreated CSAC, CSAC treated by sodium hydroxide, ammonium hydroxide, and nitric acid at approximately 17.5 min, followed by the CSAC treated by phosphoric acid and sulfuric acid at 15 and 12.5, respectively. A possible reason could be that the acid treatment resulting in a shorter time to

equilibrate the adsorbent surface with respect to carbon dioxide. Thus, the weakly adsorbed component, methane, may be displaced faster by strongly adsorbed component, carbon dioxide. As the surface treatment method on the CSAC by ammonium hydroxide has the highest BET surface area (Table 4.2), the CSAC is likely to have better physical adsorption capacity. In addition, it has a larger pore volume than the others. The adsorption capacity of the CSAC treated with sulfuric acid, phosphoric acid, and nitric acid decreases considerably due to its lower BET surface area, which may be due to the pore enlargement and surface destruction during the acid treatment. In 2005, Guo and coworkers studied the chemical activation of activated carbon with sulfuric acid. The PSAC prepared by the use of sulfuric acid as an activating agent suggested their potential applications in gas adsorption by the internal surface area development concept, which causes its relatively large micropore surface area. Moreover, in 2005, Wu and coworkers studied the development of the activated carbon surface by the chemical activation of activated charcoal with potassium hydroxide. It was found that potassium hydroxide could develop micropores, which can enhance the adsorption of methane and carbon dioxide. Under the alkaline environment, it is expected to have the formation of oxygen functional groups on the surface of activated carbon. In 2012, Olivares-Marín and coworkers also studied the surface treatment of activated carbon. The activated carbon from cherry stones was prepared by the method of physical activation in air, followed by the chemical activation in sulfuric acid. It was found that after chemical treatment, sulfuric acid yielded the activated carbon with a lower level of inorganic matters. Several factors may jointly influence overall performance of the studied carbon. Besides surface area and pore size, carbon surface chemistry might contribute significantly to adsorption capacity. Oxidation by acids or alkalis removed mineral elements and emerged other atoms. A similar phenomenon was observed in a study by Shen *et al.*, (2008). More oxygen emerged after modified by acid, indicating the addition of oxygen-containing functional groups. However, the variation of other elements had less influence on methane adsorption ability in this study. Significantly, more oxygen was detected in all acid modified CSAC compared with untreated CSAC, leading to a hydrophilic surface and disadvantage to the hydrophobic methane uptake.

The CSAC treated by MES for hydrophobic surface improvement was used to study the competitive adsorption of 10 vol% methane and 10 vol% carbon dioxide. The breakthrough curves of methane and carbon dioxide were plotted in terms of concentration ratio versus time, as shown in Figures 4.31 to 4.34.

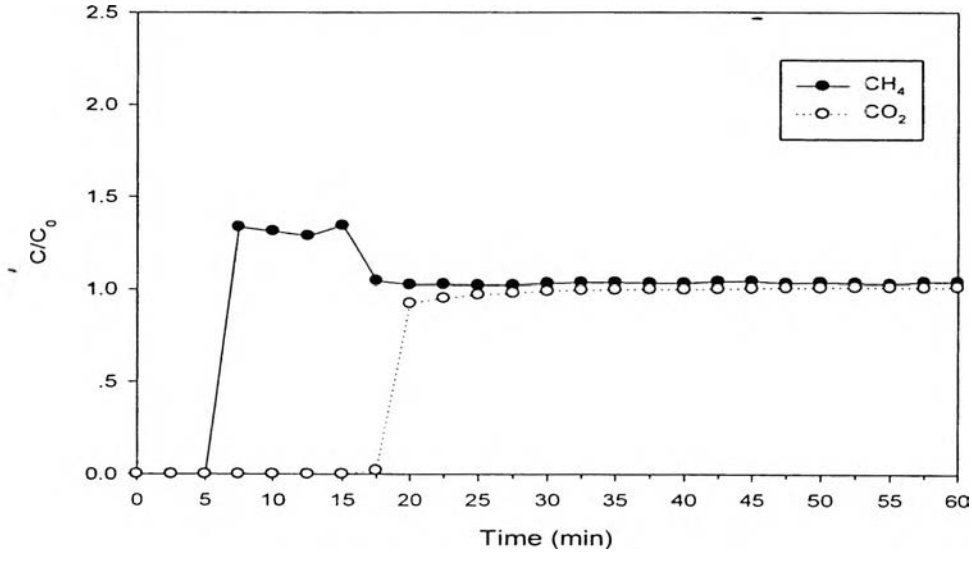

Figure 4.31 Breakthrough curves of methane and carbon dioxide from the competitive adsorption on the CSAC treated by MES at 15 mg/l with the initial concentration of methane at 10 vol% and carbon dioxide at 10 vol% at room temperature.

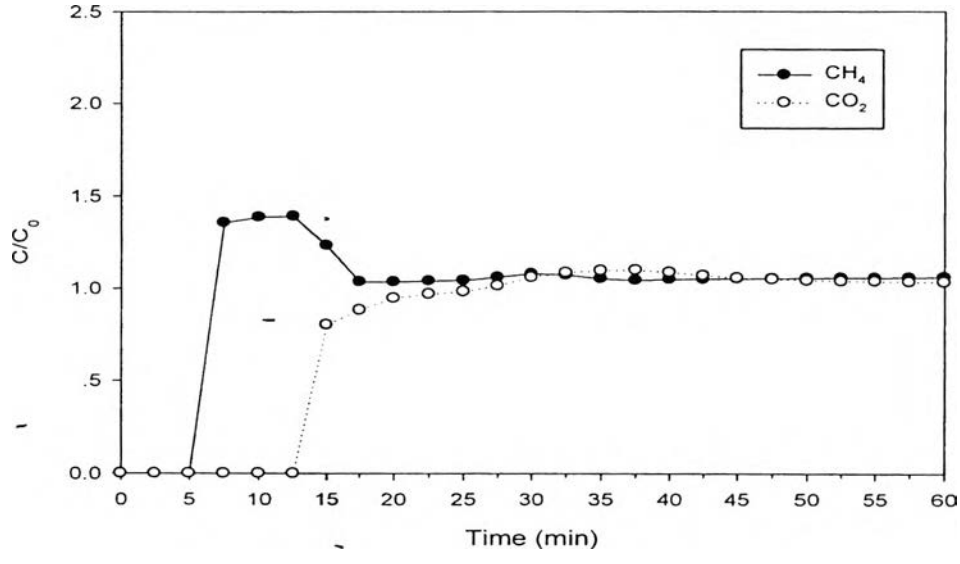

Figure 4.32 Breakthrough curves of methane and carbon dioxide from the competitive adsorption on the CSAC treated by MES at 50 mg/l with the initial concentration of methane at 10 vol% and carbon dioxide at 10 vol% at room temperature.

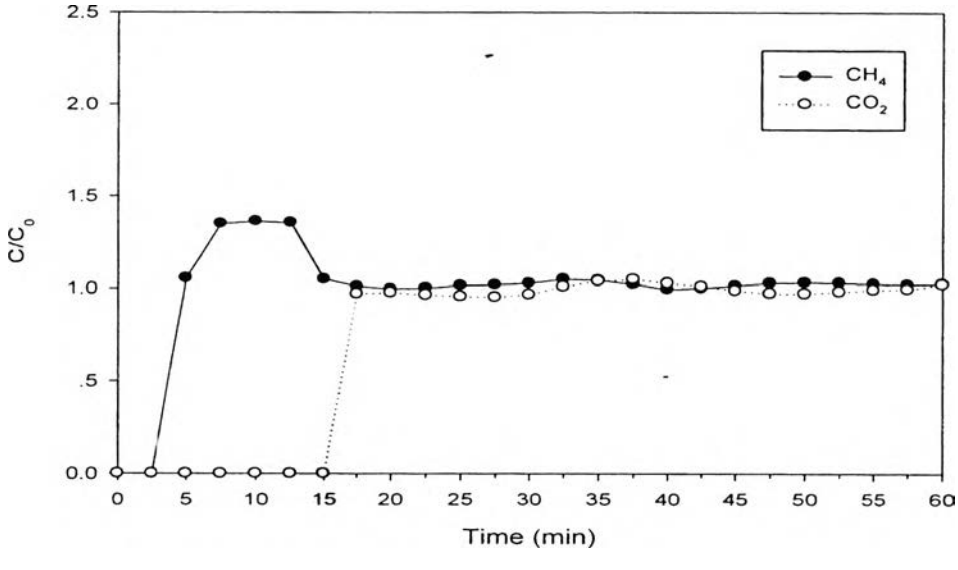

Figure 4.33 Breakthrough curves of methane and carbon dioxide from the competitive adsorption on the CSAC treated by MES at 152.8 mg/l with the initial concentration of methane at 10 vol% and carbon dioxide at 10 vol% at room temperature.

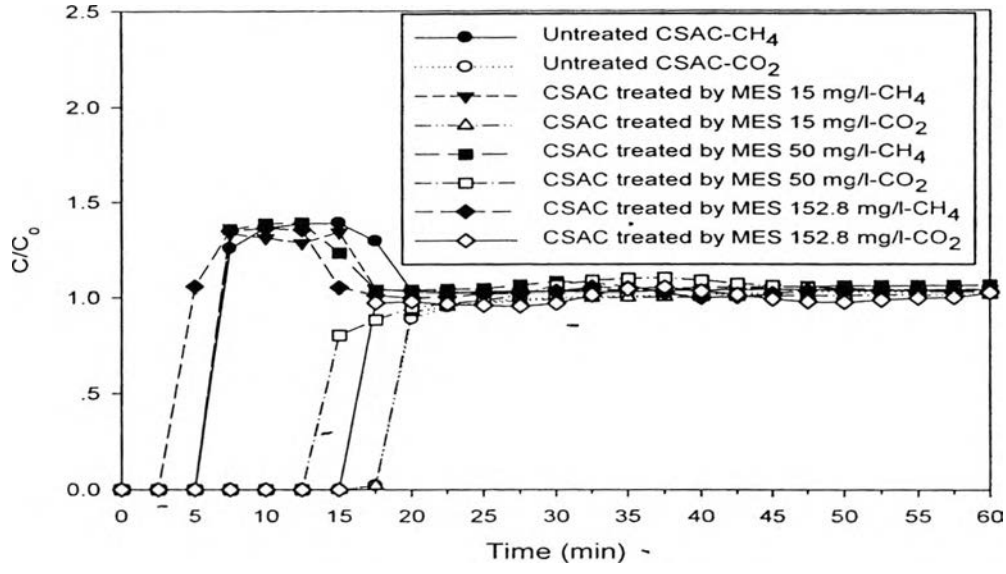

Figure 4.34 Breakthrough curves of methane and carbon dioxide from the competitive adsorption on the untreated CSAC, CSAC treated by MES at 15mg/l, 50 mg/l, and 152.8 mg/l with the initial concentration of methane at 10 vol% and carbon dioxide at 10 vol% at room temperature.

The CSAC sample was treated by MES at 15 mg/l, 50 mg/l, and 152.8 mg/l. For detail comparison, all results from Figures 4.31 to 4.33 were plotted in Figure 4.34. From Figure 4.34, it can be seen that methane breaks through first at about 2.5 min from the CSAC treated by MES at 152.8 mg/l, followed by the untreated CSAC at about 5 min. Methane elutes from the CSAC treated by MES at 15 mg/l and 50 mg/l at the same time as that of CSAC. The carbon dioxide breakthrough time is decreased subsequently from the adsorption on the untreated CSAC and CSAC treated by 15 mg/l of MES at 17.5 min to the adsorption on CSAC treated by 152.8 mg/l and 50 mg/l of MES, at 15 min and 12.5 min respectively. The decrease in the carbon dioxide adsorption on the CSAC treated with MES at 50 mg/l in comparison to the untreated CSAC and CSAC treated with 15 mg/l suggests a cumulative effect, which entails the ability to sufficiently cover the activated carbon surface with a maximum surface layer of surfactant (Mark *et al.*, 2011). Moreover, the CSAC treated MES at 50 mg/l has higher methane adsorption than the CSAC treated MES at 152.8 mg/l. A possible reason could be that the sulfonate treatment at

152.8 mg/l resulting in a shorter time to equilibrate the adsorbent surface with respect to methane. Also, the surfactant molecules adsorbed at high concentrations have a tendency to form bilayer. And because of the hydrophobic reaction between the hydrocarbon chains in this bilayer, it is claimed that the hydrophobicity transform to hydrophilicity (Zeng *et al.*, 2001). Apart from this, it is also claimed that, at high concentrations, the repulsive forces among the surfactant molecules adsorption in the interface of the solid (adsorbent)-solution are more effective (Bremmell *et al.*, 1999). And the drop in hydrophobicity is attributed to adsorption with some of the hydrophilic surface resulting in the increase in the carbon dioxide adsorption by decreasing the weakly adsorption of methane.

- 4.2.5 CH_4 and CO_2 Adsorption Capacity

The adsorption capacity was estimated from the breakthrough curves using Eq. (4.1):

$$n_{adsi} = \frac{Ft_{ni}C_{0i}}{W} \quad , \tag{4.1}$$

where n_{adsi} is the dynamic adsorption capacity of any gas i, F is the total molar flow, C_{0i} is the concentration of the gas i entering the column, W is the mass of adsorbent loaded in the column, and t_{ni} is the stoichiometric time corresponding to gas i, which is estimated from the breakthrough profile according to Eq. (4.2) (Geankoplis, 1993).

$$t_{ni} = \int_0^t \left(1 - \frac{C_{Ai}}{C_{0i}}\right) dt \quad , \tag{4.2}$$

where C_{0i} and C_{Ai} are the concentrations of any gas i upstream and downstream the column, respectively.

After determining the adsorption capacity of CO_2 and CH_4, the ideal selectivity of the adsorbent as its ability criterion in adsorption process was calculated using Eq. (4.3)

$$\text{Adsorption selectivity} = \frac{n_{CH_4}}{n_{CO_2}} \quad (4.3)$$

Table 4.6 Summary of breakthrough time, adsorption capacity, and selectivity of investigated CSAC

Adsorbent	Breakthrough time (min)		Total adsorption (mmol/g)	CH_4 adsorption (mmol/g)	CO_2 adsorption (mmol/g)	CH_4/CO_2 selectivity
	CH_4	CO_2				
CSAC	3.46	17.00	3.42	0.58	2.84	0.20
CSAC/H_2SO_4	1.76	14.64	2.73	0.29	2.44	0.12
CSAC/H_3PO_4	2.26	16.53	3.14	0.38	2.76	0.14
CSAC/HNO_3	2.22	20.19	3.74	0.37	3.37	0.11
CSAC/KOH	4.91	21.80	4.46	0.82	3.64	0.23
CSAC/NH_4OH	5.24	19.51	4.13	0.87	3.25	0.27
CSAC/NaOH	4.60	19.41	4.01	0.77	3.24	0.24
CSAC/MES at 15 mg/l	3.92	18.97	3.81	0.65	3.16	0.21
CSAC/MES at 50 mg/l	3.18	12.80	2.66	0.53	2.13	0.25
CSAC/MES at 152.8 mg/l	2.21	17.00	3.21	0.37	2.84	0.13

From Table 4.6, the breakthrough time shows that methane comes out first at 1.76 to 2.26 min of CSAC treated by acids and MES at 152.8 mg/l. The untreated CSAC, CSAC treated by alkalis and CSAC treated by MES at 15-50 mg/l, have the CH_4 breakthrough time between 3.18 and 5.24 min. Carbon dioxide, more strongly adsorbed component, has longer breakthrough time than methane. For the CSAC, the total adsorption capacity is 3.41 mmol/g with 0.58 mmol/g (6.94%) methane and 2.84 mmol/g (93.06%) carbon dioxide. The adsorption capacity of methane decreases dramatically from 0.58 mmol/g to between 0.29 and 0.38 mmol/g, after the acid treatment. The decrease is consistent with the BET surface area results. On the contrary, the methane adsorption capacity of the CSAC treated with alkalis increases from 0.58 mmol/g to 0.77, 0.82 and 0.87 mmol/g for CSAC/NaOH, CSAC/KOH, and CSAC/ NH_4OH, respectively. It was reported that the oxygen-

containing group and the surface was decreased after an alkali treatments including H_3PO_4, HNO_3, and $NH_3.H_2O$ (Li *et al.*, 2011). That may be a reason why the methane adsorption on the CSAC/NaOH, CSAC/KOH, and CSAC/ NH_4OH increases. The adsorption selectivity of CH_4/CO_2 on the investigated adsorbents shows that CSAC/ NH_4OH has the highest selectivity. Interestingly, the modification of the CSAC surface treated with MES results in the hydrophobicity of the surface and high CH_4/CO_2 selectivity as well. The results are in good agreement with that for Zor (2004).